On The Impact of Communication Delays on Power System Automatic Generation Control Performance

Jiangmeng Zhang and Alejandro. D. Domínguez-García
University of Illinois at Urbana-Champaign Urbana, Illinois 61801
Email: {jzhang67, aledan}@illinois.edu

***Abstract*—In this paper, we investigate the impact of communication delays on the performance of power system automatic generation control (AGC). To this end, we formulate a hybrid system model that describes the power system electromechanical behavior, including the AGC system dynamics. Through linearization and discretization, this hybrid system model is converted into a discrete-time linear time-invariant system model that includes the effect of delays in the AGC system communication channels. The stability of the closed-loop system can then be determined by examining the characteristics of the state-transition matrix of the aforementioned discrete-time linear system. Interesting findings include that increasing communication delay may help decrease the largest eigenvalue magnitude of the state-transition matrix. However, in reality, the delay is not constant or deterministic. We carefully analyze the stability of systems with random communication delays and nonzero mean random disturbances. The proposed analysis methodology is illustrated and verified through numerical examples.**

I. Introduction

The motivation for this work lies in the tight coupling between cyber and physical components that, under visions such as the US Department of Energy Smart Grid [1], are likely to become more prevalent in electric power systems. With increased integration of information technology (IT) systems, there is a concern that electric grids could become more vulnerable if emerging behaviors introduced by the close interaction between cyber and physical components are not carefully understood. Automatic generation control (AGC), as the only system-level automatic closed-loop control system over the IT infrastructure of a power system [1], is sensitive to such emerging behaviors, which, in turn, could have an impact on system metrics, e.g., frequency deviations from its nominal value. The AGC system takes measurements of frequency and interchange power between balancing areas as inputs, and sends out control signals to generators through the IT infrastructure. The goal of the AGC system is to regulate electrical frequency, and maintain the interchange power between balancing areas to scheduled values.

Specialized communication network and protocols in power system have received considerable attention in the context of the smart grid vision. Supervisory control and data acquisition (SCADA) systems, as computer-controlled systems, has been widely utilized in power systems for monitoring, control and protection. Furthermore, with the urge to enhance system situational awareness, as well as the availability of advanced measurement technologies, the wide area measurement system (WAMS) has been under rapid development. This system will facilitate the understanding and management of the increasingly complex behavior exhibited by large power systems. The advanced measurement devices in WAMS, called synchronized phasor measurement units (PMUs), can measure both phase magnitudes and angles at high sampling rates. In 2019, more than 1000 PMUs will be installed in North America, covering all 200 kV and above substations, and even part of the distribution network [2]. In this regard, reliable, secure, and low-latency communication network infrastructures are critical in both systems.

The Distributed Network Protocol (DNP3) is the communication protocol used in SCADA systems; the specifics of DNP3 for SCADA systems in electric power networks can be found in [3]. A protocol for synchrophasor measurement communication used in WAMS was defined in IEEE standard in 1995, and revised as IEEE Standard C37.118 in 2005 [4]. Both DNP3 and the synchrophasor measurement communication protocol mainly specify the application layer structures, and suggest Ethernet with the user datagram protocol (UDP) or transmission control protocol (TCP)/Internet protocol (IP) as lower layers of the communication network partially due to its dominance in the marketplace. However, since TCP/IP is not particularly designed for networked control systems, the potential impact on power system performance needs to be carefully studied. In [5], we studied the impact of measurement noise on power system AGC performance. In this paper, we focus on studying the impact of communication delays, which arises from network traffic or malicious attacks.

Due to the discrete nature of the sampling process in AGC, the electromechanical behavior of a power system can be modeled as a hybrid system containing a continuous-time subsystem describing the physical layer dynamics, and a discrete-time subsystem describing the dynamics of the AGC algorithms. Various approaches to analyze such hybrid system models have been explored. One common step is to formulate a consistent discrete-time system; specifically, through discretization with the same time interval as in the discrete-time subsystem, the continuous-time subsystem can be reformulated as a discrete-time subsystem. Then, by linearizing, one can study the stability of the overall system. When communication delays are considered, the system state at the next time step does not only depend on the control command in the previous time step, but also on the second to last command. This can be captured during the discretization process by dividing the time interval into two parts, the time before the new command arrives and the time after. Note that generally, there are frequency-domain and time-domain methods to address the impact of time delays on system performance. For instance, [6] proposed a frequency-domain method to evaluate such impact on automatic voltage regulators and power system stabilizers. However, the hybrid nature of the AGC system, as well as the uncertainty on the time delays introduced from the communication network, makes the frequency-domain method not applicable in this study.

Although some network protocols guarantee a constant communication delay, most protocols, such as TCP/IP, introduce varying delays. The work in [7] considered a system with delays taking values in a finite set, and studied its stability. The work in [8] studied a real-time control system with random delays obeying independent probabilistic distributions; the stability of the system with zero mean disturbance was analyzed. The work in [9] experimentally measured and analyzed the delay errors in an Ethernet-based communication infrastructure for power systems. The work in [10] studied the impact of communication delays on electricity markets.

In this paper, we propose a framework to evaluate the impact of communication delays on power system AGC performance. The electromechanical behavior of the power system, including the AGC, is modeled as a hybrid system. We then linearize each subsystem comprising the hybrid system using the same technique used in [11]. Disturbances to the linearized system model are introduced as variable loads. Note that uncertain renewable generation can also be captured by treating it as a negative load. Building on this hybrid system model, and adopting the discretization process in [7], [8], an augmented discrete-time system can be formulated. Due to the large number of communication delay causes, which can occur randomly, it is reasonable to model delays as independent random variables obeying normal distributions. In order to analyze the stability of the system, dynamic equations of the state first and second moments are formulated. Particularly, the nonzero mean disturbance (i.e., variable load) makes the stability analysis for systems with zero mean disturbance in [8] not applicable, and entails careful input-to-state stability analysis. In this work, we will derive a stability criterion for such systems with nonzero mean disturbance.

The remainder of this paper is organized as follows. In Section II, we formulate the electromechanical behavior of the power system including the effect of AGC, as a nonlinear hybrid system, which we then linearize and reformulate as an LTI discrete-time system. In Section III, we evaluate the impact on the system performance of both deterministic and random communication delays. Section IV illustrates the analysis methodology via numerical examples. Concluding remarks and future work are presented in Section V.

II. Preliminaries: Power System Model with AGC

In this section, we introduce the modeling framework adopted in this work. The power system electromechanical dynamics is modeled as a set of continuous differential algebraic equations (DAEs), while the AGC system dynamics is described via a discrete-time state-space model. The resulting hybrid model is then reformulated as a discrete-time linear system through discretization and linearization.

A. Power System Model with AGC

1) Electromechanical dynamics: We use the standard DAE model to describe the power system electromechanical behavior. Let $x(t) \in \mathbb{R}^a$ denote a vector that contains the dynamic states of synchronous generators; $y(t) \in \mathbb{R}^b$ denote the system algebraic states, including bus voltage magnitudes and angles; and $p(t) \in \mathbb{R}^c$ denote the loads. Then, the power system electromecahnical behavior can be described by a set of DAEs of the form:

$$\dot{x}(t) = f(x(t), y(t), u(t)), \tag{1a}$$

$$0 = g(x(t), y(t), p(t)), \tag{1b}$$

where $u(t) \in \mathbb{R}^d$ contains the generator set points that are determined by the AGC algorithm as described below. The function $f : \mathbb{R}^{a+b+d} \rightarrow \mathbb{R}^a$ captures the evolution of the dynamic states. A nine-state machine model can be used for representing the dynamics of individual generators [12], and correspondingly, nine dynamic states for each synchronous generator will be included in $x(t)$.

Following [13], we adopt a reduced-order model, which only includes the mechanical equations and the governor dynamics, i.e., for each generator, only the rotor electrical angular position, angular velocity and mechanical torque are included in $x(t)$. Note that the rotor angle position of a particular synchronous generator is chosen as the reference, and all other angles are defined relative to it. Therefore, there are only two dynamic states associated with this particular synchronous generator. The function $g : \mathbb{R}^{a+b+c} \rightarrow \mathbb{R}^b$ models the electrical network.

2) AGC system: Consider a power system with M balancing authority (BA) areas indexed by $\mathcal{A} = \{1, 2, \cdots, M\}$. For every $m \in \mathcal{A}$, $\mathcal{A}_m \subset \mathcal{A}$ denotes the set of BA areas that are connected to area m through tie lines. The objective of AGC is to maintain (i) the real power interchange between BA areas to the scheduled values, and (ii) the system frequency to its nominal value. This is achieved by minimizing the area control error (ACE) of each BA area. The ACE for area m is calculated as

$$ACE_m = \sum_{n \in \mathcal{A}_m} (P_{mn} - P_{mn}^{sch}) - b_m(f_m - f_{nom}),$$

where $b_m > 0$ is the bias factor for area m; P_{mn} denotes the actual power interchange from area m to its neighboring area n, while P_{mn}^{sch} denotes the scheduled value; and f_m is the actual system frequency, while f_{nom} is the nominal system frequency. The value of P_{mn} can be obtained by summing over the real power flow of the tie lines from area m to area n, and f_m can be obtained by taking a weighted sum of the frequencies on the buses in area m.

A new dynamic state, z_m, for area m is used to capture the AGC behavior. Measurements are taken at discrete time instants; we denote the sample interval as Δt, and define $z_m[k] := z_m(k\Delta t)$ and $ACE_m[k] := ACE_m(k\Delta t)$. Let $\mathcal{G}_m$ denote the set of generators in area m that participate in AGC. Then, the dynamics of $z_m[k]$ is described by

$$z_m[k+1] = z_m[k] + \Delta t(-z_m[k] + ACE_m[k] + \sum_{i \in \mathcal{G}_m} P_{S_i}[k]),$$

where $P_{S_i}[k] = P_{S_i}(k\Delta t)$, $i \in \mathcal{G}_m$, is the power output of generator i at instant $k\Delta t$.

For each generator $i \in \mathcal{G}_m$, the set point at instant k, denoted by $P_{C_i}[k]$, is determined as a function of $z_m[k]$ as follows: $P_{C_i}[k] = \kappa_{m_i} z_m[k]$, where the κ_{m_i}'s are called the participation factors and satisfy $\sum_{i\in\mathcal{G}_m} \kappa_{m_i} = 1$, for any $m \in \mathcal{A}$. Then, the set points for all the generators in all BA areas form the vector $u[k]$, i.e., $u[k] = \{P_{C_i}[k]\}$, for each $i \in \mathcal{G}_m$ and each $m \in \mathcal{A}$. Define $z[k] = [z_1[k], z_2[k], \cdots, z_M[k]]^T$, $x[k] = x(k\Delta t)$, and $y[k] = y(k\Delta t)$; and note that the bus frequency is the derivative of the bus voltage angle with respect to time, while the bus voltage angle is the element of y. Therefore, f_m can be obtained by computing $\dot{y}$. Then, the AGC system can be described in a compact form as

$$z[k+1] = h_1(z[k],\, x[k],\, y[k],\, \dot{y}[k]), \tag{2a}$$
$$u[k] = h_2(z[k]). \tag{2b}$$

The set points stay constant during the sample interval, i.e.,

$$u(t) = u[k],\; k\Delta t \le t < (k+1)\Delta t.$$

B. Linearization

Assume that the hybrid system model in (1) and (2) evolves towards an equilibrium point (x^*, y^*, z^*, u^*) under a certain load profile p^*. Let $x(t) = x^* + \Delta x(t)$, $y(t) = y^* + \Delta y(t)$, $z[k] = z^* + \Delta z[k]$, and $u[k] = u^* + \Delta u[k]$, where $\Delta x(t), \Delta y(t), \Delta z[k]$ and $\Delta u[k]$ result from the change in the load profile $\Delta p(t) = p(t) - p^*$. Assume the disturbance $\Delta p(t)$ is sufficiently small, such that $\Delta x(t), \Delta y(t), \Delta z[k]$ and $\Delta u[k]$ are sufficiently small. By linearizing (1) and (2) around (x^*, y^*, z^*, u^*), we obtain a set of linear equations of the form

$$\begin{aligned}
\Delta\dot{x}(t) &= A_1\Delta x(t) + A_2\Delta y(t) + B_1\Delta u(t), && \text{(3a)}\\
0 &= A_3\Delta x(t) + A_4\Delta y(t) + C_1\Delta p(t), && \text{(3b)}\\
\Delta z[k+1] &= A_5\Delta x[k] + A_6\Delta y[k] + A_7\Delta\dot{y}[k]\\
&\quad + B_2\Delta z[k], && \text{(3c)}\\
\Delta u[k] &= B_3\Delta z[k], && \text{(3d)}
\end{aligned}$$

where $\Delta x[k] = \Delta x(k\Delta t)$, $\Delta y[k] = \Delta y(k\Delta t)$, and $A_1 - A_7$, $B_1 - B_3$ and C_1 are matrices obtained from the partial derivatives of the functions f, g, h_1, and h_2 evaluated at the equilibrium point.

Assume that invertability of matrix A_4 always holds; then, by substituting $\Delta y(t)$ and $\Delta u(t)$ into (3a) and (3c), we can obtain a hybrid model of the form

$$\Delta\dot{x}(t) = A_9\Delta x(t) + B_4\Delta z(t) + C_2\Delta p(t), \tag{4a}$$
$$\Delta z[k+1] = A_{10}\Delta x[k] + B_5\Delta z[k] + C_3\Delta p[k], \tag{4b}$$

where

$$\begin{aligned}
A_9 &= A_1 - A_2A_4^{-1}A_3,\\
A_{10} &= A_5 - A_6A_4^{-1}A_3 + A_7A_4^{-1}A_3(A_4^{-1}A_3 - A_1),\\
B_4 &= B_1B_3,\; B_5 = B_2 - A_7A_4^{-1}A_3B_1B_3,\\
C_2 &= -A_2A_4^{-1}C_1,\; C_3 = -A_6A_4^{-1}C_1;
\end{aligned}$$

$\Delta p[k] = \Delta p(k\Delta t)$; and $\Delta z[k] = \Delta z(k\Delta t)$ for $k\Delta t \le t < (k+1)\Delta t$. Note that $\Delta\dot{y}(t)$ can be expressed as a linear function of $\Delta\dot{x}(t)$, which in turn is a linear combination of $\Delta x(t), \Delta y(t)$ and $\Delta u(t)$. Therefore, we can evaluate the derivative of $\Delta y(t)$ as a linear combination of $\Delta x(t)$ and $\Delta u(t)$. Another way to circumvent the use of $\Delta\dot{y}(t)$ is to represent the deviation in the area frequency as the electrical speed deviation of the generators in the area, which are a subset of the elements of $\Delta x(t)$. Therefore, $\Delta f_m(t)$ can be expressed as a linear function of $\Delta x(t)$; then, $\Delta\dot{y}(t)$ will not appear; and $B_5 = B_2$. The accuracy of this approximation has been verified via simulations in [14].

C. Discretization

Next, we convert the hybrid system in (4) into a discrete-time linear system. To this end, (4b) is discretized as follows,

$$\Delta x[k+1] = \Phi_1\Delta x[k] + \Gamma_1\Delta z[k] + \Gamma_2\Delta p[k], \tag{5}$$

where

$$\Phi_1 = e^{A_9\Delta t},\; \Gamma_1 = \int_0^{\Delta t} e^{A_9 s}\mathrm{d}sB_4,\; \Gamma_2 = \int_0^{\Delta t} e^{A_9 s}\mathrm{d}sC_2.$$

Combining (4) and (5), we obtain a linear discrete-time model of the form

$$X_n[k+1] = \Phi_n(\Delta t)X[k] + C_n(\Delta t), \tag{6}$$

where $X_n[k] = [\Delta x[k]^T,\, \Delta z[k]^T]^T \in \mathbb{R}^{a+M}$; and $\Phi_n(\Delta t)$ and $C_n(\Delta t)$ are defined as

$$\Phi_n(\Delta t) = \begin{bmatrix} \Phi_1 & \Gamma_1 \\ A_{10} & B_5 \end{bmatrix},\, C_n(\Delta t) = \begin{bmatrix} \Gamma_2\Delta p[k] \\ C_3\Delta p[k] \end{bmatrix}.$$

D. Stability

Given that $C(\Delta t)$ is bounded, the stability of the system in (6) can be determined by the eigenvalues of $\Phi_n(\Delta t)$ [15]. The system is stable when the largest eigenvalue magnitude is less than 1, otherwise, the system will diverge under any disturbance. Note that as discussed in Section II-B, the matrix B_5 in $\Phi_n(\Delta t)$ can be approximated by $B_2 = (1 - \Delta t)I_M$, where I_M is an identity matrix of size M. Therefore, although the open-loop system without AGC is stable, meaning that the magnitudes of all eigenvalues of Φ_1 are less than 1, a relatively large Δt may lead the largest eigenvalue magnitude of $\Phi_n(\Delta t)$ to be larger than 1. Also, since it is determined by B_5, the largest eigenvalue magnitude of $\Phi_n(\Delta t)$ should be monotonic with respect to Δt. This will be illustrated in Section IV.

III. Assessing the Impact of Communication Delays

In this section, an augmented discrete-time model is formulated taking into account the delay in communication channels. Then, by using the augmented discrete-time model in (6), we analyze the impact on the system stability of both deterministic and random communication delays.

A. Deterministic Communication Delay

In (4), assume that the sample interval Δt is constant. For $k \in \mathbb{Z}^+$, at time $k\Delta t$, the frequency and generators' outputs are measured and transmitted from the local measurement devices to the control center; let d_1 denote the time delay during this process. After the AGC system receives the measurements, it will calculate the new generator set point $u[k]$, and send $u[k]$ to the generators participating in AGC; let d_2 denote the corresponding communication delay time. Assume that the measuring time and computing time are negligible comparing to the communication delay. The command will be received by generators at time $k\Delta t + d_1 + d_2$, meaning that the total time delay is $d = d_1 + d_2$. Until this new command arrives, the generators use the previous set point value $u[k-1]$. Assume that $d \leq \Delta t$, then the set point values $u(t)$ used by the generators are

$$u(t) = \begin{cases} u[k-1], & k\Delta t \leq t < k\Delta t + d, \\ u[k], & k\Delta t + d \leq t < (k+1)\Delta t. \end{cases} \tag{7}$$

1) Discretization: Given (7), the commands passed to the generators are no longer constant during each time interval $[k\Delta t, (k+1)\Delta t]$. We partition this interval into two parts: $[k\Delta t, k\Delta t + d]$ and $[k\Delta t + d, (k+1)\Delta t]$, and discrete (4a) over each of these two intervals:

$$\begin{aligned} \Delta x(k\Delta t + d) &= \Phi_2 \Delta x(k\Delta t) + \Gamma_3 \Delta z[k-1] \\ &\quad + \Gamma_4 \Delta p(k\Delta t),\ k\Delta t \leq t \leq k\Delta t + d \end{aligned} \tag{8a}$$

$$\begin{aligned} \Delta x((k+1)\Delta t) &= \Phi_3 \Delta x(k\Delta t + d) + \Gamma_5 \Delta z[k] \\ &\quad + \Gamma_6 \Delta p(k\Delta t + d),\ k\Delta t + d \leq t \leq (k+1)\Delta t \end{aligned} \tag{8b}$$

where

$$\Phi_2 = e^{A_9 d},\ \Phi_3 = e^{A_9(\Delta t - d)},$$
$$\Gamma_3 = \int_0^d e^{A_9 s} \mathrm{d}s B_4,\ \Gamma_4 = \int_0^d e^{A_9 s} \mathrm{d}s C_2,$$
$$\Gamma_5 = \int_0^{\Delta t - d} e^{A_9 s} \mathrm{d}s B_4,\ \Gamma_6 = \int_0^{\Delta t - d} e^{A_9 s} \mathrm{d}s C_2.$$

Substituting (8a) into (8b), and assuming that the disturbance is constant during one sample interval, we obtain that

$$\Delta x[k+1] = \Phi_1 \Delta x[k] + \Gamma_5 \Delta z[k] + \Gamma_7 \Delta z[k-1] + \Gamma_2 \Delta p[k],$$

where

$$\Phi_1 = e^{A_9 \Delta t},\ \Gamma_5 = A_9^{-1}[e^{A_9(\Delta t - d)} - I]B_4,$$
$$\Gamma_7 = A_9^{-1}[e^{A_9 \Delta t} - e^{A_9(\Delta t - d)}]B_4,\ \Gamma_2 = A_9^{-1}[e^{A_9 \Delta t} - I]C_2.$$

Define $X[k] = [\Delta x[k]^T, \Delta z[k]^T, \Delta z[k-1]^T]^T$; then, we have that

$$X[k+1] = \Phi(\Delta t, d) X[k] + C, \tag{9}$$

where

$$\Phi(\Delta t, d) = \begin{bmatrix} \Phi_1 & \Gamma_5 & \Gamma_7 \\ A_{10} & B_2 & 0 \\ 0 & I_{M\times M} & 0 \end{bmatrix},\ C = \begin{bmatrix} \Gamma_2 \Delta p[k] \\ C_3 \Delta p[k] \\ 0 \end{bmatrix}.$$

Note that Φ is function of Δt and d. For an ideal communication network (i.e., $d = 0$), $\Gamma_7 = 0$. Then, the model in (9) is reduced to the model in (6).

2) Stability: Since the time delay d is assumed to be deterministic for now, $\Phi(\Delta t, d)$ is also deterministic. The stability of this system is determined by the largest magnitude of the eigenvalues of $\Phi(\Delta t, d)$. Note that although the sample interval Δt is properly designed to make the system in (6) stable, certain communication delays can cause the system in (9) to become unstable. Moreover, unlike the monotonic relationship between Δt and the largest eigenvalue magnitude, the relationship between the time delay d and the largest eigenvalue magnitude is non-monotonic. Thus, an increase in the communication delay may help mitigate the instability of the system. Similar findings have been presented in [10], where the authors analyzed the impact of the communication delay on the performance of electrical markets; this phenomenon will be illustrated in Section IV.

B. Random Communication Delay

In reality, communication delays may vary at each instant $k\Delta t$. Due to the large number of factors that affect the communication delay, including various waiting time depending on the network traffic, and retransmission due to transmission errors, it is reasonable to model the delays as normally distributed random variables. As in [8], we also assume independence on the communication delays across time; therefore, by taking expectations on both sides of (9), we obtain

$$\mathbb{E}[X[k+1]] = \mathbb{E}[\Phi(\Delta t, d)]\mathbb{E}[X[k]] + \mathbb{E}[C], \tag{10}$$

where $\mathbb{E}[C]$ is bounded.

1) Stability: If the largest eigenvalue magnitude of $\mathbb{E}[\Phi(\Delta t, d)]$ is larger than 1, $\mathbb{E}[X[k]]$ will diverge with k. However, even if the largest eigenvalue magnitude is less than 1, this does not necessarily guarantees that the system is stable almost surely. Note that during the calculation of $\mathbb{E}[\Phi(\Delta t, d)]$, the exponential function of a normal random variable appears; this expectation can be evaluated by utilizing the moment generating function of a normal distribution.

For a random process, mean square stability implies almost sure stability [8]. Therefore, in order to investigate the system stability, we examine the dynamics of the state second moment, which is described by

$$\begin{aligned} \mathbb{E}[X[k+1]X[k+1]^T] &= \mathbb{E}[(\Phi X[k] + C)(\Phi X[k] + C)^T] \\ =&\mathbb{E}[\Phi X[k] X[k]^T \Phi^T] + \mathbb{E}[\Phi]\mathbb{E}[X[k]]\mathbb{E}[C^T] \\ &+ \mathbb{E}[C]\mathbb{E}[X[k]^T]\mathbb{E}[\Phi^T] + \mathbb{E}[CC^T]. \end{aligned} \tag{11}$$

One way to analyze the stability of the system in (11) is to collect the first and second moments into an augmented vector. To this end, define $P[k] = [\mathbb{E}[X[k]X[k]^T], \mathbb{E}[X[k]]]$, and convert $P[k]$ into a column vector. Then, we obtain that

$$\mathrm{vec}(P[k+1]) = G_1 \mathrm{vec}(P[k]) + G_2,$$

where G_1 and G_2 can be determined from (10) and (11). However, in this case, G_1 contains the elements of the vector C, which are unknown but bounded. Therefore, the eigenvalues of matrix G_1 will be underdetermined. This underdetermination can be circumvented by considering the mean and the second moments separately; this idea is captured in Lemma 1.

Lemma 1. *For the system*

$$X[k+1] = \Phi X[k] + C,$$

where C is bounded, second moment stability can be determined by the largest eigenvalue magnitude of $\mathbb{E}[\Phi \otimes \Phi]$, where $\otimes$ indicates Kronecker products.

Proof: The proof consists of two parts. The first part is to show that if $\mathbb{E}[\Phi \otimes \Phi]$ is Schur (i.e., all its eigenvalues' magnitudes are less than one), then $\mathbb{E}[\Phi]$ is Schur. Note that this is not trivial and cannot be explicitly proven by directly applying the spectrum property of the Kronecker product (i.e., the eigenvalues of a matrix squared are equal to the squares of the eigenvalues of this matrix [7], [8]). Because $\mathbb{E}[\Phi \otimes \Phi]$ is not equal to $\mathbb{E}[\Phi] \otimes \mathbb{E}[\Phi]$. However, we can prove this by examining a special case where $C = 0$. In this case, convert the second moment matrix into a column vector. Then, the second moment evolves according to

$$\mathrm{vec}(\mathbb{E}[X[k+1]X[k+1]^T]) = \mathbb{E}[\Phi \otimes \Phi]\mathrm{vec}(\mathbb{E}[X[k]X[k]^T]).$$

If $\mathbb{E}[\Phi \otimes \Phi]$ is Schur, then this system is second-moment stable, and subsequentally almost surely stable. Therefore, the mean converges as well. On the other side, because the mean evolves according to

$$\mathbb{E}[X[k+1]] = \mathbb{E}[\Phi]\mathbb{E}[X[k]],$$

then, $\mathbb{E}[\Phi]$ has to be Schur so that the mean converges.

In the second part, we consider the general case where C is not equal to zero, but bounded. Let

$$G_3 := \mathbb{E}[\Phi]\mathbb{E}[X[k]]\mathbb{E}[C^T] + \mathbb{E}[C]\mathbb{E}[X[k]^T]\mathbb{E}[\Phi^T] + \mathbb{E}[CC^T].$$

Then, the mean and the second moment evolve according to

$$\mathbb{E}[X[k+1]] = \mathbb{E}[\Phi]\mathbb{E}[X[k]] + \mathbb{E}[C], \tag{12a}$$

$$\mathrm{vec}(\mathbb{E}[X[k+1]X[k+1]^T]) = \mathbb{E}[\Phi \otimes \Phi]\mathrm{vec}(\mathbb{E}[X[k]X[k]^T]) + \mathrm{vec}(G_3). \tag{12b}$$

Because $\mathbb{E}[\Phi]$ is Schur and $\mathbb{E}[C]$ is bounded, then, from (12a), we conclude that $\mathbb{E}[X[k]]$ is bounded. Then, we obtain that G_3 is bounded as well. Given (12b), $\mathbb{E}[\Phi \otimes \Phi]$ being Schur can guarantee the convergence of the second moment. ■

By using Lemma 1, it is straightforward to show that the almost sure stability of the system in (9) can be determined by the largest eigenvalue magnitude of $\mathbb{E}[\Phi \otimes \Phi]$.

IV. Case Study

In this section, we illustrate the proposed analysis framework with a 4-bus system. Two synchronous generators, one renewable generation unit and one load comprise this power system model. A complete list of its dynamic and static parameters, as well as the AGC parameters, can be found in [5], [14]. The electromechanical behavior of each synchronous machine is described by a third-order model (see e.g., [13]). Since one of the rotor angles is chosen as reference, we have that $x(t) \in \mathbb{R}^5$. The disturbance to the dynamics is introduced by varying the load. The AGC signal is sampled every two seconds.

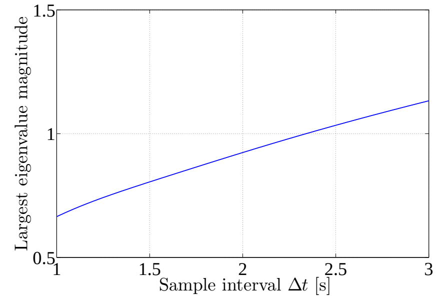

Figure 1: Eigenvalues v.s. sample interval.

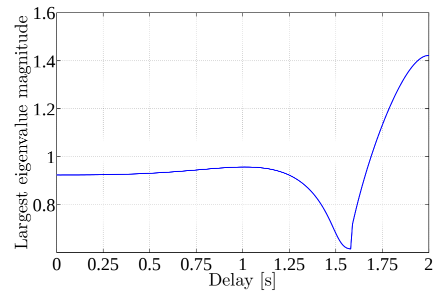

Figure 2: Eigenvalues v.s. communication delays.

First, as discussed in Section II-D, Fig. 1 illustrates the monotonic relationship between the sample intervals and the largest eigenvalue magnitudes. This figure also illustrates that although the original system with AGC is stable, large AGC sample interval may cause system instability. Next, we investigate the impact of deterministic communication delays. Figure 2 depicts the largest eigenvalue magnitudes as we vary the communication delay. For a certain range, the largest eigenvalue magnitude decreases as the delay is increased. The system is stable until the delay is larger than 1.70 s. Figure 3, which presents one generator's rotor speed, verifies that the system is still stable when the delay is 1.70 s. Simulations with both linear and nonlinear models are conducted, and the good matching of the results verifies the effectiveness of the linear model.

Next, we investigate the impact of random delays. First, we assume that the random delay has a mean of 0.2 s. Figure 4(a) depicts the largest eigenvalue magnitude as we vary the variance, from which we can observe that the system is robust to

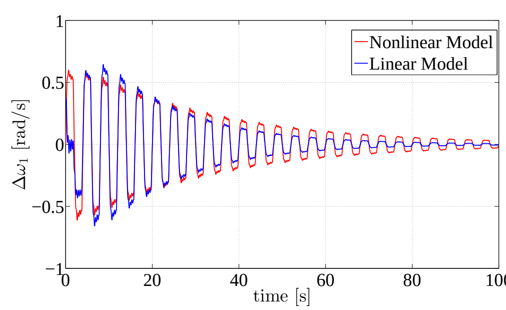

Figure 3: Simulation with 1.7 s deterministic delay.

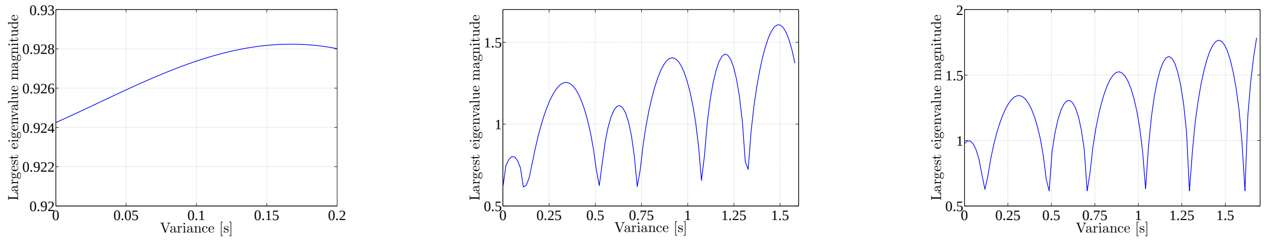

(a) Eigenvalue v.s. variance with a mean of 0.2 s. (b) Eigenvalue v.s. variance with a mean of 1.60 s. (c) Eigenvalue v.s. variance with a mean of 1.70 s.

Figure 4: Eigenvalue v.s. variance.

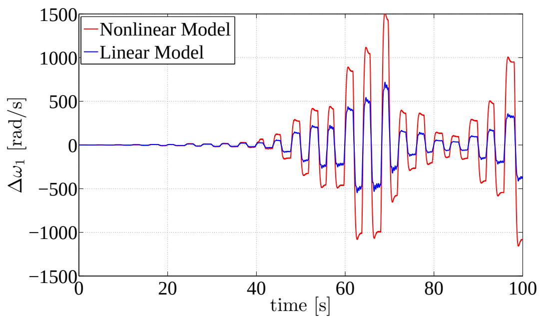

Figure 5: Simulation at 1.7 s delay with 0.02 s^2 variance.

variance variation when the delay is relatively small. However, when the delay has a relatively large mean, the system stability is less robust to variance variation. For instance, we consider the case when the mean of delay is 1.60 s, which corresponds to the lowest largest eigenvalue magnitude in Fig. 2 with deterministic delays. However, Fig. 4(b) demonstrates that the system tends to be unstable with very small variance.

An extreme case is when the mean of the delay is 1.7 s, with which the system is stable if the variance is zero. Figure 4(c) shows that the system becomes unstable with a variance of 0.02 s^2. The simulation results, as presented in Fig. 5, confirm that the system diverges when the delay has a mean of 1.7 s and a variance of 0.02 s^2; the rotor speed deviation achieves unrealistic values in 60 s.

V. Concluding Remarks

This paper proposed a framework to investigate the impact of communication delay on power system AGC performance. With this framework, we can determine whether the delay in the communication network, caused by natural traffic or malicious attacks, remain within acceptable ranges to maintain system stability. We achieve this by modeling the system dynamics with AGC algorithm as a hybrid system, converting it to a linear discrete-time system, and examining the eigenvalues of the system matrix. Particularly, when the delay is assumed to be random, we proposed a stability criterion for the resulting random system with nonzero mean disturbance.

We illustrate this methodology in several case studies. Insightful observations include that the largest eigenvalue magnitude of the system matrix may be decreased as the deterministic communication delay increases. However, although large deterministic delay may help improve the system stability, small variance on the delay may cause system instability.

This framework is also applicable to other cyber-physical systems, such as distributed control system. This framework can also be generalized to cases where multiple measurements and commands are transmitted through multiple communication channels with different delays, and the delays may be modeled as a Markov chain.

References

[1] A. Bose, "Models and techniques for the reliability analysis of the smart grid," in *Proc. of IEEE Power and Energy Society General Meeting*, July 2010.

[2] North American SynchroPhasor Initiative, "Synchrophasor technology roadmap," March 2009.

[3] "IEEE standard for electric power systems communications-distributed network protocol (dnp3)," *IEEE Std 1815-2012 (Revision of IEEE Std 1815-2010)*, pp. 1–821, Oct 2012.

[4] "IEEE standard for synchrophasors for power systems," *IEEE Std C37.118-2005 (Revision of IEEE Std 1344-1995)*, pp. 1–57, 2006.

[5] J. Zhang and A. D. Domínguez-García, "On the failure of power system automatic generation control due to measurement noise," in *Proc. of IEEE Power and Energy Society General Meeting*, Jul 2014.

[6] F. Milano and M. Anghel, "Impact of time delays on power system stability," *Circuits and Systems I: Regular Papers, IEEE Transactions on*, vol. 59, no. 4, pp. 889–900, April 2012.

[7] J. Hespanha, P. Naghshtabrizi, and Y. Xu, "A survey of recent results in networked control systems," *Proceedings of the IEEE*, vol. 95, no. 1, pp. 138–162, Jan 2007.

[8] J. Nilsson, "Real-time control systems with delays," Ph.D. dissertation, Lund Institute of Technology, 1998.

[9] S. Carullo and C. Nwankpa, "Experimental validation of a model for an information-embedded power system," *IEEE Transactions on Power Delivery*, vol. 20, no. 3, pp. 1853–1863, July 2005.

[10] J. Nutaro and V. Protopopescu, "The impact of market clearing time and price signal delay on the stability of electric power markets," *IEEE Transactions on Power Systems*, vol. 24, no. 3, pp. 1337–1345, Aug 2009.

[11] Y. Chen and A. Domínguez-García, "A method to study the effect of renewable resource variability on power system dynamics," *IEEE Transactions on Power Systems*, vol. 27, no. 4, pp. 1978–1989, Nov 2012.

[12] P. W. Sauer and M. A. Pai, *Power System Dynamics and Stability*. Upper Saddle River, NJ: Prentice Hall, 1998.

[13] A. Domínguez-García, *Control and Optimization Methods for Electric Smart Grids, Power Electronics and Power Systems*. Springer, 2012, vol. 3, pp. 149–165.

[14] D. Apostolopoulou, Y. Chen, J. Zhang, A. Domínguez-García, and P. Sauer, "Effects of various uncertainty sources on automatic generation control systems," in *Proc. of IREP Symposium*, Aug 2013.

[15] E. D. Sontag, "Input to state stability: Basic concepts and results," in *Nonlinear and Optimal Control Theory*. Springer, 2006, pp. 163–220.